ORIGINAL ARTICLE

Laplace-Based Interpolation Method in Reduction of Metal Artifact in Computed Tomography Imaging

Noor Diyana Osman[1], Nurul Fathin Mohamad Sobri[1], Anusha Achuthan[1,2], Mohd Norsyafi Hassan[3], Muhamad Zabidi Ahmad[1], Mohd Zahri Abdul Aziz[1]

[1] Advanced Medical and Dental Institute, Universiti Sains Malaysia, Kepala Batas, 13200, Penang, Malaysia;
[2] School of Computer Science, Universiti Sains Malaysia, Minden, 11800, Penang, Malaysia;
[3] Department of Diagnostic Imaging, Hospital Limbang, Jalan Pandaruan, Limbang, 98700, Sarawak, Malaysia

ABSTRACT

Introduction: Metal artifacts can degrade the image quality of computed tomography (CT) images which lead to errors in diagnosis. This study aims to evaluate the performance of Laplace interpolation (LI) method for metal artifacts reduction (MAR) in CT images in comparison with cubic spline (CS) interpolation. **Methods:** In this study, the proposed MAR algorithm was developed using MATLAB platform. Firstly, the virtual sinogram was acquired from CT image using Radon transform function. Then, dual-adaptive thresholding detected and segmented the metal part within the CT sinogram. Performance of the two interpolation methods to replace the missing part of segmented sinogram were evaluated. The interpolated sinogram was reconstructed, prior to image fusion to obtain the final corrected image. The qualitative and quantitative evaluations were performed on the corrected CT images (both phantom and clinical images) to evaluate the effectiveness of the proposed MAR technique. **Results:** From the findings, LI method had successfully replaced the missing data on both simple and complex thresholded sinogram as compared to CS method (p-value = 0.17). The artifact index was significantly reduced by LI method (p-value = 0.02). For qualitative analysis, the mean scores by radiologists for LI-corrected images were higher than original image and CS-corrected images. **Conclusion:** In conclusion, LI method for MAR produced better results as compared to CS interpolation method, as it worked more effective by successfully interpolated all the missing data within sinogram in most of the CT images.
Malaysian Journal of Medicine and Health Sciences (2022) 18(6):243-250. doi:10.47836/mjmhs18.6.32

Keywords: Computed tomography, Image segmentation, Metal artifact reduction, Sinogram interpolation

Corresponding Author:
Noor Diyana Osman, PhD
Email: noordiyana@usm.my
Tel: +604-5622421

INTRODUCTION

CT examination involving patient with metal objects which are present in CT images may give rise to streak artifact in CT images. The metal-induced artifacts appear as dark and bright lines emanating from the metal objects that may obscure the anatomical details around the metal objects on the CT image. In the presence of severe artifacts, image quality may be extensively degraded and important clinical findings and pathology in the vicinity of the metal objects may be obscured. The sources of the artifacts are due to beam hardening effects, photon starvation, scatter, and noise due to the attenuation by dense objects, and inaccurate reconstruction algorithm (1-3).

Several approaches have been proposed to reduce the appearance of metal artifacts in CT images. The simplest methods include discarding metal objects from the field-of-view (FOV) during scanning, modification of image acquisition and reconstruction such as increasing kVp and mAs settings, using sharp kernel and extended CT-scale (ECTS) technique, gantry tilt angulation and dual-energy acquisition (4-10). The more complicated methods used post-processing algorithms which typically involve the use of mathematical solution such as filtering, interpolation and iterative reconstruction technique. The earliest method was introduced by Kalendar et al. in 1987 that was known as image-based approach (11).

The more recent correction algorithm involves post-processing technique that were applied on the raw image data (sinogram) and resulted in more accurate metal artifacts reduction (MAR). In more recent study, the MAR is applied in both sinogram and image domains and has showed significant reduction of artifacts (12). The proposed algorithms can be categorized into two groups which are sinogram interpolation (SI) and

iterative reconstruction (IR) (9). In iterative reconstruction methods, the projection data associated to dense objects are disregarded, and these values are replaced by projections estimations and the reconstruction is applied only for non-corrupted data based on image assumptions (13-16). The IR algorithm are more accurate and reliable for incomplete and noisy projection data as compared to SI method.

Recently, deep learning-based algorithm (deep MAR) has been proposed which is either applied on projection (DLP-MAR) or image (DLI-MAR) domains, or combinations of both domains known as dual-domain MAR (17-20). The deep MAR methods trained the deep network using both real and simulated datasets. Du et al., (2021) reported that the major problem with deep MAR methods is the domain gap problem which resulted in insufficient solution for metal artifact especially on dental dataset (18).

However, the interpolation method is the most widely implemented for MAR as it is much more straightforward and less computationally expensive as compared to IR technique (9, 21). The sinogram interpolation (SI) technique is also known as projection completion. The SI technique directly corrects or replaces the corrupted projection data (due to metal object) in the sinogram domain by interpolation method. The replacement values are interpolated either from neighboring projections or from a mathematical model (22). Few interpolation methods have been proposed in previous studies such as polynomial interpolation, linear interpolation, wavelet interpolation, interpolation by contouring, cubic spline interpolation and sinogram inpainting (11, 21, 23-25). The interpolation process is computationally efficient, but it often generates new artifacts in the final images due to the interpolation errors (26).

The main limitation with SI approach is inaccurate segmentation problem that usually appear as under-segmentation and over-segmentation of metal trace within the sinogram or projection data (18). In our previous studies, it has also been reported that the artifacts were not completely removed, or additional artifacts may be introduced due to incomplete interpolation of the projection data or sinogram (27-28). The missing data were not fully replaced in CT image with severe artifact that consist multiple or complex shaped metal objects. In this paper, two sinogram interpolation technique were investigated and the efficiency of both SI approach in the reduction of artifacts in CT imaging were evaluated using both quantitative and qualitative analysis. The cubic spline (CS) interpolation technique from our previous work were compared with the proposed Laplace-based interpolation (LI) techniques. The Laplace interpolation method is preferable because this method selects the smoothest possible interpolant among all possible partial differential solutions (29-30).

MATERIALS AND METHODS

MAR Method

The proposed artifact correction technique consists of three main steps: (1) metal segmentation, (2) sinogram interpolation and (3) image reconstruction (as shown in Figure 1). Firstly, virtual sinogram, go was acquired from the original CT image, fo using Radon transform function. This technique was proposed by Abdoli et al., (2010) and it is preferable as it is simpler, and the correction was performed directly on projection data in sinogram domain (31). The first step is the thresholding technique to identify the corrupted data affected by the metal artifact and segment the metal region within the CT sinogram. Metal segmentation was performed directly in sinogram, which is more efficient than performing segmentation on reconstructed images. The segmentation is achieved by using the dual-step adaptive thresholding (DSAT) technique (27). In this technique, two threshold values were determined, which were threshold value of metal (T1) and threshold value of metal + bone (T2), as shown in Figure 1. The DSAT technique is based on local adaptive thresholding that selects an individual threshold for metal pixel based on the range of highest intensity values in its local neighborhood. The second thresholding, T2 was applied to retain the surrounding bone structures affected by metal artifacts on the final image.

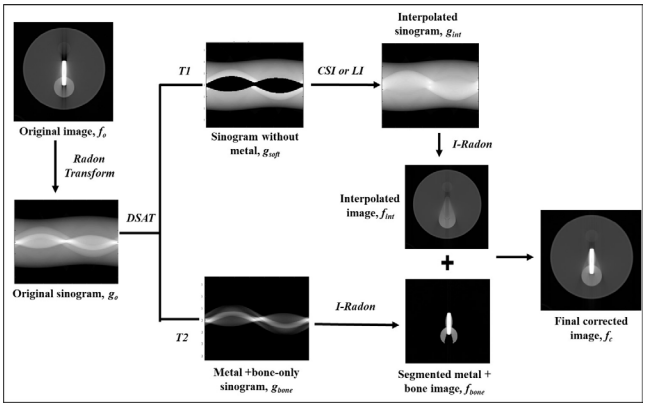

Figure 1:The overview of the proposed MAR algorithm

The second step is the sinogram interpolation (SI) method performed within the missing data of the segmented metal region in the thresholded sinogram. During interpolation, the segmented region is replaced by new values using an interpolation scheme. Two interpolation methods were applied and investigated, namely cubic spline (CS) and Laplace interpolation (LI) techniques. CS interpolation works by replacing the missing sinogram data using four neighboring pixels within the projection at each projection angle. In the LI method, pixels in the segmented region (missing data) were corrected using smooth interpolation from the surrounding pixels using the Laplace's equation:

$$\frac{d^2\varphi}{dx^2} + \frac{d^2\varphi}{dy^2} = 0 \quad (1)$$

The LI method uses inward interpolation from the pixel values on the outer boundary of the metal regions, g_{metal}. This algorithm computes the discrete Laplacian over regions and solves the Dirichlet boundary value problem. In Dirichlet problems, the LI function on the metal region boundary is equal to harmonic function, φ.30 Finally, the interpolated sinogram, g_{int} was reconstructed using back-projection method that was calculated by inverse Radon transform, in prior to image fusion. The metal+bone segmented image, f_{bone} was fused with the interpolated image, f_{int} to obtain the final corrected image, f_c (as shown in Figure 1).

Images Collection

For verification of the MAR algorithm, CT data of phantom images and clinical CT images consist of different severity of metal artifacts were included in the study. A customized phantom from previous study was used to simulate the corrupted images due to metal-induced artifacts.27 The phantom images consist of different positions of metal insertions and quantities of metal inserts (single and multiple rods) to simulate different artifacts severity. Both phantom and clinical CT images were scanned and acquired using the Siemens SOMATOM Definition AS+ CT Scanner (Siemens Healthcare, Germany) at Imaging Unit, Advanced Medical and Dental Institute (AMDI), Universiti Sains Malaysia (USM), Penang and Department of Radiology, Hospital USM (HUSM), Kelantan, Malaysia.

For clinical images, a total of 7 images were archived and selected retrospectively from Picture Archiving and Communication System (PACS), at both centers using non-randomized purposive sampling. The clinical images were selected according to their degree of severity of metal streaks due to different metal implant such as hip prosthesis, spinal and surgical screws. This study has been approved by the human ethical committee of our university (Approval no. USM/JEPEM/16020045) for clinical data study. All CT images were reconstructed using a smooth kernel.

Objective Image Analysis

The performance of the two interpolation, CS and LI methods to replace the missing part of thresholded sinogram were evaluated. The MAR validation was performed by evaluating the results of both interpolation methods qualitatively and quantitatively. Quantitative image analysis was performed using region of interest regions of interest (ROIs) statistical analysis at CT workstation. Few ROIs were drawn at few selected points within the artifact regions, and the mean and standard deviation (SD) of CT attenuation values in Hounsfield unit (HU) were measured. The artifacts index (AI) for each image was calculated to compare the effectiveness of both interpolation methods. The AI is defined as below (32-33):

$$AI = \sqrt{SD^2_{ROI\,(metal)} - SD^2_{ROI(ref)}} \quad (2)$$

AI is calculated based on SD values determined at ROIs near metal artifacts, $SD_{ROI(metal)}$ and reference images without metal artifacts, $SD_{ROI(ref)}$ in phantom images. The calculated AI for both SI techniques were compared. A paired T-test was performed to determine the significant differences between both SI methods by calculating the statistical *p*-value.

Subjective Image Analysis

The qualitative assessment was performed using a blinded scoring technique that was carried out by two experienced radiologists with more than 5 years of experience in CT imaging. All the images were blinded and randomly organized during the qualitative evaluation by the radiologists. The two radiologists (R1 and R2) were also blinded to the exposure parameters and system protocols. The images were evaluated using the same window settings (soft-tissue window). Qualitative improvement was assessed and compared on the original images with artifacts and corrected clinical images (by both SI methods).

The radiologists scored all the clinical images independently by using a 4-point score based on previous studies (34-36). The blinded scoring was based on two characteristics of image quality which the degree and appearance of metal artifacts were evaluated based on score from 0 to 3 (0 = severe and prominent artifacts, 1 = artifacts are present but less prominent, 2 = minor and faint artifacts, and 3 = no artifacts). The second characteristic is the conspicuity of anatomical structures adjacent to metal implants that was scored from 0 to 3 (0 = totally obscured, no or questionable anatomic recognition, 1 = minor visibility or faint anatomic recognition, 2 = anatomic recognition with low confidence in potential diagnosis, and 3 = anatomic recognition with high confidence in potential diagnosis). The statistical analysis was performed by determining the inter-observer agreement for subjective analysis using Cohen's Kappa test. The results are classified as follows: poor (κ < 0.20); fair (κ = 0.21-0.40); moderate (κ = 0.41-0.60); good (κ = 0.61-0.80) and excellent agreement (κ = 0.81-1.00) (32). A negative kappa represents agreement worse than expected, or no agreement. The Kruskal-Wallis test was also conducted for further statistical analysis on non-parametric qualitative image assessment. The significant differences between the mean scores between both SI techniques were determined.

RESULTS

Objective Image Analysis

From the findings, it can be observed that different SI techniques performed differently in replacement of the missing data in the segmented sinogram, gsoft of the phantom images (as shown in Fig.2). Figure 2 shows the comparison of interpolated sinogram between CS and LI method on few selected phantom images. The interpolation performance is depending on the severity of the artifacts which is influenced by the shape and numbers of metal inserts in the original image, f_o. In Figure 2, single metal rod will have simple sinogram and multiple rods will produce complex shape of sinogram, g_o. Both CS and LI methods are capable of successfully replaced all the missing data on simple segmented sinogram, g_{soft} (as observed in phantom 1) in Figure 2. However, for more severe artifacts and complicated sinogram (as observed on phantom 2 and 3), LI method works more effectively by fully interpolated the missing data, $g_{LI\text{-}int}$ as compared to CS method, $g_{CS\text{-}int}$ (Fig. 2).

From the quantitative analysis on phantom images, the calculated SNR values for CS-corrected images were higher compared to LI-corrected images. These demonstrate that CS method produced image with less noise as compared to LI method. Figure 3 plotted the artifact index (AI) values for all corrected phantom images (by both CS and LI methods) in comparison with the original images. From this figure, it can be observed that most of the calculated AI values for LI-corrected images is lower than the original image, but few CS-corrected images have higher AI than the original images. The mean ± SD of AI values obtained were 99.31 ± 44.57 (original image), 141.43 ± 119.41 (CS-corrected image), and 66.07 ± 23.89 (LI-corrected image). From the statistical analysis, it shows that the differences of AI values between original and LI-corrected images were statistically significant (p-value = 0.02), but there is no significant difference of AI values between original and CS-corrected images (p-value = 0.17).

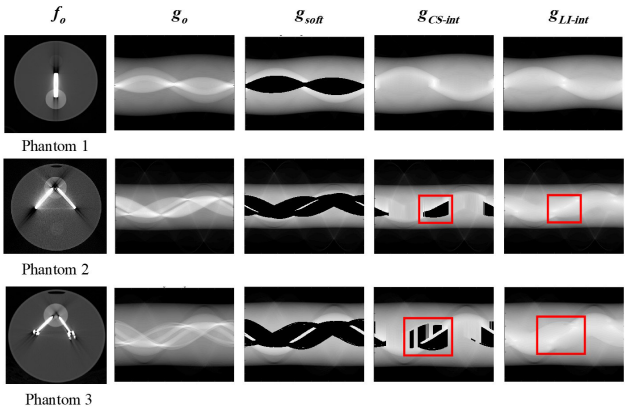

Figure 2: Comparison of the interpolated sinogram using CS and LI methods on phantom images.

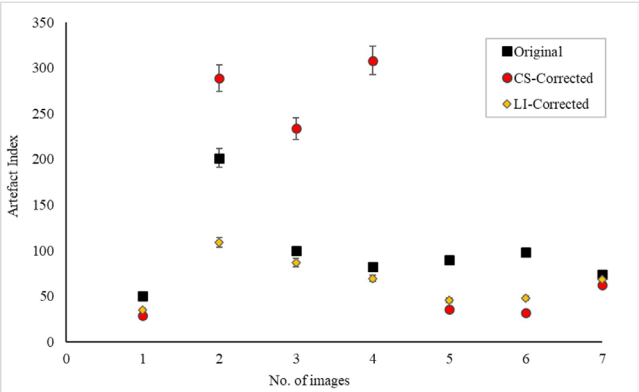

Figure 3: Graph of artefacts index (AI) for original images and corrected images by both CS and LI methods

Subjective Image Analysis

Figure 4 shows the comparison of the original with both CS-corrected and LI-corrected images of few selected clinical CT images due to different metal prosthesis. From this figure, it can be observed that the corrected clinical images by LI method produced better image quality with reduced artifacts appearance as compared to CS method, except for clinical image 3. In both clinical image 1 and 2, CS method shows severe new artifacts introduced in the final corrected images (second row of Fig. 4). The qualitative image analysis was evaluated using blinded scoring techniques between two radiologists, known as R1 and R2.

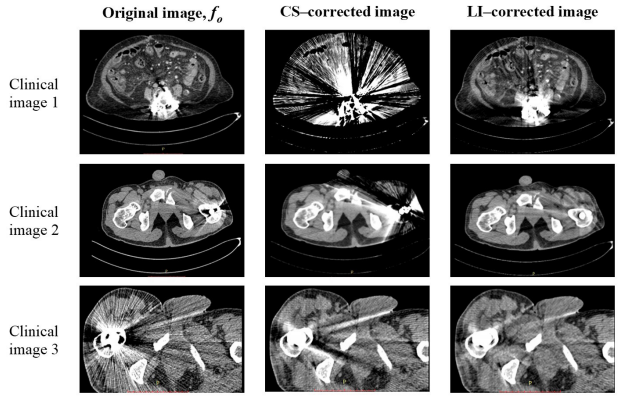

Figure 4: Comparison of the original and corrected clinical images by both CS and LI methods.

The results for agreement between the two radiologists were obtained using Cohen's Kappa test. From the results, it shows that there was no agreement between R1 and R2 scoring for the original image with low negative value (κ = -0.286). For corrected clinical images, there were moderate agreement between the scoring of the two radiologists for CS method (κ = 0.429) and fair agreement between for LI method (κ = 0.205) for the first characteristics of image quality. For second characteristics, there was disagreement between both radiologists scoring for the original image with low negative value (κ = -0.340). For corrected clinical images, there were moderate agreement between both

radiologists for CS method (κ = 0.571) and fair agreement for LI method (κ = 0.308).

For qualitative evaluation, the images were scored based on two characteristics: (1) conspicuity of the adjacent structures and (2) the appearance of metal artifacts. The quality scores (mean ± SD) given by both radiologists (R1 and R2) using the blinded scoring technique were summarised in Table I. The scores for different characteristics were also plotted for comparison, as shown in Fig. 5 and 6. For conspicuity of the adjacent structures, the mean ± SD of the scores were 1.08 ± 1.08, 1.33 ± 1.23, and 1.75 ± 1.22 for original, CS-corrected and LI-corrected images, respectively. The average score for LI method is higher than CS method, which indicates better image quality produces by LI method. This proved that LI method work more effectively in the reduction of metal artifacts on the clinical images as compared to CS method. For comparative study between original and corrected images (by both SI), there is no significant different on the visibility of the anatomical structures adjacent to the metal prosthesis with p-value of 0.70 and 0.30 for CS and LI methods, respectively.

For second characteristics which is evaluation of the appearance of the metal artifacts, the mean ± SD of the image scores were 0.25 ± 0.45 (original); 1.08 ± 1.00 (CS-corrected) and 1.08 ± 0.79 (LI-corrected). From the results, it shows that the corrected images by both methods showed higher image scores as compared to original image. For comparative study between original and corrected images (by both SI), there is no significant different on the visibility of the metal-induced artifacts between original and CS-corrected images, with p-value of 0.08. However, the difference between original and LI-corrected images is statistically significant (p = 0.04).

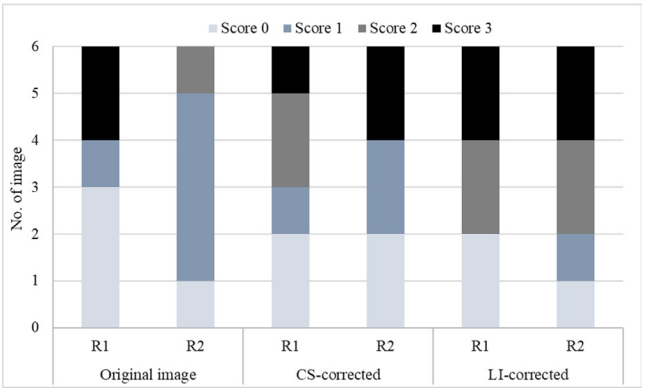

Figure 5: Distribution of scores by both radiologist (R1 and R2) for evaluation of conspicuity of adjacent structures.

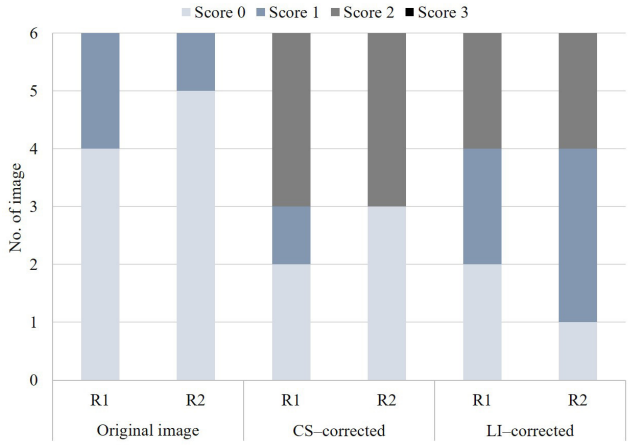

Figure 6: Distribution of scores by both radiologists (R1 and R2) for the appearance of metal artefacts.

DISCUSSION

From the results, it can be observed that both interpolation; CS and LI methods work well on simple thresholded sinogram or less severe artifacts (Phantom 1) by fully interpolating the missing data, as shown in Figure 3. However, for more complicated sinogram with severe metal artifacts (Phantom 2 and 3), the CS method was less effective and not capable to fully interpolate the missing data in sinogram (in Figure 3). These will lead

Table I: The quality scores (mean ±SD) using the blinded scoring technique by both radiologists (R1 and R2) based on the quality criteria

Clinical Images	Image Scores & Evaluation Criteria											
	Conspicuity of the adjacent structures						Appearance of metal artefacts					
	Original		CS-corrected		LI-corrected		Original		CS-corrected		LI-corrected	
	R1	R2	R1	R2	R1	R2	R1	R2	R1	R2	R1	R2
1	1	2	0	0	0	1	0	1	0	0	0	1
2	3	1	0	0	3	3	1	0	0	0	2	2
3	0	1	1	1	0	0	0	0	1	2	0	0
4	3	1	2	1	3	2	1	0	2	0	2	1
5	0	1	3	3	2	2	0	0	2	2	1	1
6	0	0	2	3	2	3	0	0	2	2	1	2
Mean ± SD	1.08 ± 1.08		1.33 ± 1.23		1.75 ± 1.22		0.25 ± 0.45		1.08 ± 1.00		1.08 ± 0.79	

to incomplete projection data within the sinogram that will induce new artifact on the final corrected images. In contrast, the LI method is more effective and capable to fully interpolate the segmented sinogram as compared to CS method. Both quantitative and qualitative analysis on the corrected images supported that Laplace-based interpolation is superior as compared to CS interpolation and well-known as perfect interpolator with smooth interpolation. Studies done by Veldkamp et al., (2009,2010) also showed that Laplace interpolation gives better and more consistent results in artifacts suppression (26, 30).

The quantitative results showed that most of the mean AI values for LI-corrected images is lower than original image (Figure 3). This indicates that LI method images yield lower noise with reduced artifact as compared to original images. Lower AI values for all LI-corrected images proved that this technique resulted in improved image quality and did not produce new artifact on the final corrected image due to full interpolation of the missing data (as shown in Figure 2). In contrast, the mean AI values for some of the CS-corrected images are higher than the original image which shows that this method is less effective in interpolation of the missing sinogram data and also induced new artifacts on final corrected images. In this study, significant reduction of AI by 33% was demonstrated after the application of the LI technique.

For all clinical images, the radiologists judged the original and corrected images for visibility of artifacts and relevant anatomical structures adjacent to the metal implant. From the qualitative analysis, the average scores by both radiologists for the corrected images of both SI methods are significantly higher than the original image. This proved that the corrected images produced improved quality with suppressed artifacts as compared to the original images. Both radiologists noticed improved image quality due to reduction of the bright and dark streaks originating from the metal implant. In more detail, this appeared to result in substantially improved anatomical structures adjacent to the implant. The comparative study between both SI methods resulted in higher mean score for LI-corrected images than CS-corrected images for conspicuity of the adjacent structures. This demonstrated that LI method are better and work more effectively for the reduction of metal artifacts on the clinical images as compared to CS method. As compared to the CS-corrected images, the LI-corrected images have superior uniformity in known ROIs and improved the visual definition of structures.

In this work, we demonstrate the effectiveness and potential of our algorithm on simulated datasets using phantom images and real clinical CT datasets. This work also demonstrated the simplicity of Laplace-based interpolation that successfully replaced all the missing data due to metal trace within the segmented sinogram. It is recommended for future work to include the comparative study of our proposed technique with the more recent approach, deep learning-based MAR methods and explore the potential of combining our proposed MAR with the deep MAR method.

CONCLUSION

This study described a method to reduce the metal-induced artifacts and evaluating two sinogram interpolation methods. Our method is different because the corrupted data due to metal implant was segmented using dual-step adaptive thresholding instead of single thresholding that was based on global thresholding. The implementation of segmentation and correction directly on virtual sinogram obtained from Radon transform avoids the need for a complex computing of the original CT raw data. Moreover, our method could be potentially faster since the complex computing is omitted. In conclusion, the results of this study have demonstrated the ability of Laplace interpolation-based MAR method in suppressing metal-induced artifacts with significant improvement of image quality as confirmed by the quantitative and qualitative analysis. LI-based MAR method is superior and significantly reduced the artifacts compared to CS-based MAR method both objectively and subjectively. In summary, the LI-based MAR method is relatively a simple interpolation method that allows a significant improvement of images that are corrupted by metal artifacts.

ACKNOWLEDGEMENT

This work was funded by Universiti Sains Malaysia (USM) under the Research University (RUI) Grant (Grant No.:1001/CIPPT/811344). We would like to thank all staff at Imaging Unit, Clinical Trial Complex, Advanced Medical and Dental Institute (IPPT) USM, Penang, Malaysia and Department of Radiology, Hospital Universiti Sains Malaysia (HUSM), Kelantan, Malaysia for their help throughout the study.

REFERENCES

1. Boas, F. E., & Fleischmann, D. (2012). CT artifacts: Causes and reduction techniques. Imaging in Medicine, 4(2), 229-240. doi: 10.2217/iim.12.13
2. Yazdi, M., & Beaulieu, L. (2008). Artifacts in spiral X-ray CT scanners: problems and solutions. International J of Biological and Medical Sciences, 4(3), 135-139.
3. Barret, J. F., & Keat, N. (2004). Artifacts in CT: Recognition and avoidance. RadioGraphics. 24, 1679–1691. doi: 10.1148/rg.246045065. doi:10.5281/zenodo.1080245
4. Link, T. M., Berning W., Scherf S., Joosten U., Joist A., Engelke K., et al. (2000). CT of metal implants: reduction of artifacts using an extended CT scale technique. J. of Computer Assisted Tomography.

24(1), 165-72. doi: 10.1097/00004728-200001000-00029
5. Osman, N. D., Suhaimi, N. M., Saidun, H. A., & Razali, M. A. S. M. (2019). Metal Artefact Reduction with Different Transverse Angles of Metal Placement and Gantry Tilt Angulation in Spine CT Imaging. Mal J Med Health Sci. 15(SUPP9), 1-6.
6. Saidun, H. A., Shuaib, I. L., Daud, N. M., Sobri, N. F. M., & Osman, N. D. (2019). Evaluation of metal artefacts reduction by application of monoenergetic extrapolation of dual-energy CT: A phantom study with different metal implants. In J. of Physics: Conference Series. 1248(1), p.012004. IOP Publishing. doi: 10.1088/1742-6596/1248/1/012004
7. Bamberg, F., Dierks, A., Nikolaou, K., Reiser, M. F., Becker, C. R., and Johnson, T. R. C. (2011). Metal artifact reduction by dual energy computed tomography using monoenergetic extrapolation. Eur Radiol. 21, 1424–1429. doi: 10.1007/s00330-011-2062-1
8. Han, S. C., Chung, Y. E., Lee, Y. H., Park, K. K., Kim, M. J., Kim, K. W. (2014). Metal artifact reduction software used with abdominopelvic dual-energy CT of patients with metal hip prostheses: Assessment of image quality and clinical feasibility. American J of Radiology. 203, 788-795. doi: 10.2214/AJR.13.10980
9. Gjesteby, L., De Man, B., Jin, Y., Paganetti, H., Verburg, J., Giantsoudi, D., & Wang, G. (2016). Metal artifact reduction in CT: Where are we after four decades?. IEEE Access, 4, 5826-5849. doi:10.1109/ACCESS.2016.2608621
10. Vellarackal, A. J., & Kaim, A. H. (2021). Metal artefact reduction of different alloys with dual energy computed tomography (DECT). Scientific Reports, 11(1), 1-11. doi: 10.1038/s41598-021-81600-1
11. Kalendar, W. A., Hebel, R., and Ebersberger, J. (1987). Reduction of CT artifacts caused by metallic implants. Radiology. 164, 576-577. doi: 10.1148/radiology.164.2.3602406.
12. Lee, D., Park, C., Lim, Y. et al. (2020). A Metal Artifact Reduction Method Using a Fully Convolutional Network in the Sinogram and Image Domains for Dental Computed Tomography. J Digit Imaging, 33, 538–546. doi: 10.1007/s10278-019-00297-x.
13. Wang, G., Vannier, M. W., Cheng, P. C., et al. (1999). Iterative x-ray cone-beam tomography for metal artifact reduction and local region reconstruction. Microscopy and Microanalysis, 5(1), 58-65. doi: 10.1017/S1431927699000057.
14. Robertson, D. D., Yuan, J., Wang, G., et al. (1997). Total hip prosthesis metal-artifact suppression using iterative deblurring reconstruction. J of Comput. Assist. Tomogr., 21(2), 293-298. doi: 10.1097/00004728-199703000-00024.
15. Wang, G., Snyder, D. L., O'Sullivan, J. A., et al. (1996). Iterative deblurring for CT metal artifact reduction. IEEE Transactions in Medical Imaging, 15(5), 657-664. doi: 10.1109/42.538943.
16. Zhang, Y., Pu, Y. F., Hu, J. R., et al. (2011). Efficient CT metal artifact reduction based on fractional-order curvature diffusion. Computational and Mathematical Methods in Medicine. 173748. doi: 10.1155/2011/173748.
17. Arabi, H., & Zaidi, H. (2021). Deep learning–based metal artefact reduction in PET/CT imaging. European radiology, 31(8), 6384-6396. doi: 10.1007/s00330-021-07709-z.
18. Du, M., Liang, K., Liu, Y., & Xing, Y. (2021). Investigation of domain gap problem in several deep-learning-based CT metal artefact reduction methods. arXiv preprint arXiv:2111.12983. doi: 10.48550/arXiv.2111.12983
19. Ghani, M. U., & Karl, W. C. (2019). Fast enhanced CT metal artifact reduction using data domain deep learning. IEEE Transactions on Computational Imaging, 6, 181-193. doi: 10.1109/TCI.2019.2937221
20. Liang, K., Zhang, L., Yang, H., Yang, Y., Chen, Z., & Xing, Y. (2019). Metal artifact reduction for practical dental computed tomography by improving interpolation-based reconstruction with deep learning. Medical Physics, 46(12), e823-e834. doi: 10.1002/mp.13644.
21. Glover, G. H., & Pelc, N. J. (1981). An algorithm for the reduction of metal clip artifacts in CT reconstructions. Med Phys, 8(6), 799–807. doi: 10.1118/1.595032.
22. Rousselle, A., Amelot, A., Thariat, J., Jacob, J., Mercy, G., De Marzi, L., & Feuvret, L. (2020). Metallic implants and CT artefacts in the CTV area: Where are we in 2020?. Cancer Radiothérapie, 24(6-7), 658-666. doi: 10.1016/j.canrad.2020.06.022.
23. Zhao, S., Robeltson, D., Wang, G., Whiting, B., & Bae, K. (2000). X-ray CT metal artifact reduction using wavelets: an application for imaging total hip prostheses. IEEE Trans. on Medical Imaging, 19(12), 1238-1247. doi: 10.1109/42.897816.
24. Gu J, Zhang L, Yu G, Xing Y, Chen Z. (2006). X-ray CT metal artifacts reduction through curvature based sinogram inpainting. J. of X-Ray Science and Technology. 14(2), 73–82.
25. Meyer, E., Raupach, R., Lell, M., Schmidt, B., & Kachelrieß, M. (2010). Normalized metal artifact reduction (NMAR) in computed tomography. Med Phys, 37(10), 5482–5493. doi: 10.1118/1.3484090
26. Veldkamp, W. J. H., Joemai, R. M. S., van der Molen, A. J., Geleijns, J. (2010). Development and validation of segmentation and interpolation techniques in sinograms for metal artifact suppression in CT. Med Phys., 37(2), 620–628. doi: 10.1118/1.3276777.
27. Osman, N. D., Salikin, M. S., Saripan, M. I., Aziz, M. Z. A., Daud, N. M., (2014, December). Metal artefact correction algorithm based-on DSAT

technique for CT images. In 2014 IEEE Conference on Biomedical Engineering and Sciences (IECBES) (pp. 324-327). IEEE. doi: 10.1109/IECBES.2014.7047513

28. Osman, N. D., Sobri, N. F. M., Achuthan, A., Saidun, H. A., Aziz, M. Z. A., & Shuaib, I. L. (2018, December). Evaluation of Two Sinogram Interpolation Methods for Metal Artefacts Reduction in Computed Tomography. In 2018 IEEE-EMBS Conference on Biomedical Engineering and Sciences (IECBES). pp. 137-139. IEEE.doi: 10.1109/IECBES.2018.8626670
29. Press, W. H., Teukolsky, S. A., Vetterling, W. T., & Flannery, B. P. (2007). Numerical recipes 3rd edition: The art of scientific computing. Cambridge university press.
30. Veldkamp, W J. H., Joemai, R. M. S., & Geleijns, J. (2009). SU-FF-I-38: Automated Segmentation and Interpolation in Sinograms for Metal Artifact Suppression in CT. Med Phys, 36(6Part3), 2443-2443. doi: 10.1118/1.3181157
31. Abdoli, M., Ay, M. R., Ahmadian, A., & Zaidi, H. (2010). A virtual sinogram method to reduce dental metallic implant artefacts in computed tomography-based attenuation correction for PET. Nuclear Medicine Communications, 31(1), 22–31. doi: 10.1097/MNM.0b013e32832fa241.
32. Agrawal, N., Sinha, P., Kumar, A., & Bagai, S. (2015). Fast & dynamic image restoration using Laplace equation-based image inpainting. J Undergraduate Res Innovation, 1(2), 115-123.
33. Dong, Y., Shi, A. J., Wu, J. L., Wang, R. X., Sun, L. F., Liu, A. L., & Liu, Y. J. (2016). Metal artifact reduction using virtual monochromatic images for patients with pedicle screws implants on CT. European Spine J, 25(6), 1754-1763. doi: 10.1007/s00586-015-4053-4.
34. Yoo, H. J., Hong, S. H., Chung, B. M., Moon, S. J., Choi, J. Y., Chae, H. D., & Chang, M. Y. (2018). Metal artifact reduction in virtual monoenergetic spectral dual-energy CT of patients with metallic orthopedic implants in the distal radius. American J of Roentgenology, 1083-1091. doi: 10.2214/AJR.18.19514
35. Takayanagi, T., Suzuki, S., Katada, Y., Ishikawa, T., Fukui, R., Yamamoto, Y., & Abe, O. (2019). Comparison of Motion Artifacts on CT Images Obtained in the Ultrafast Scan Mode and Conventional Scan Mode for Unconscious Patients in the Emergency Department. American J of Roentgenology, 213(4), W153-W161. doi: 10.2214/AJR.19.21456.
36. Boas, F. E., & Fleischmann, D. (2011). Evaluation of two iterative techniques for reducing metal artifacts in computed tomography. Radiology, 259(3), 894-902. doi: 10.1148/radiol.11101782.